Multi objective Taguchi optimization approach for resistance spot welding of cold rolled TWIP steel sheets

To cite this article: Mumin Tutar *et al* 2017 *J. Phys.: Conf. Ser.* **885** 012010

IOP Conf. Series: Journal of Physics: Conf. Series **885** (2017) 012010 doi:10.1088/1742-6596/885/1/012010

Multi objective Taguchi optimization approach for resistance spot welding of cold rolled TWIP steel sheets

Mumin Tutar[1], Hakan Aydin[1], Ali Bayram[1]

[1]Uludağ University, Faculty of Engineering, Department of Mechanical Engineering, 16059, Görükle-Bursa / TURKEY

mumintutar@uludag.edu.tr

Abstract. Formability and energy absorption capability of a steel sheet are highly desirable properties in manufacturing components for automotive applications. TWinning Induced Plastisity (TWIP) steels are, new generation high Mn alloyed steels, attractive for the automotive industry due to its outstanding elongation (%40-45) and tensile strength (~1000MPa). So, TWIP steels provide excellent formability and energy absorption capability. Another required property from the steel sheets is suitability for manufacturing methods such as welding. The use of the steel sheets in the automotive applications inevitably involves welding. Considering that there are 3000-5000 welded spots on a vehicle, it can be interpreted that one of the most important manufacturing method is Resistance Spot Welding (RSW) for the automotive industry. In this study; firstly, TWIP steel sheet were cold rolled to 15% reduction in thickness. Then, the cold rolled TWIP steel sheets were welded with RSW method. The welding parameters (welding current, welding time and electrode force) were optimized for maximizing the peak tensile shear load and minimizing the indentation of the joints using a Taguchi L9 orthogonal array. The effect of welding parameters was also evaluated by examining the signal-to-noise ratio and analysis of variance (ANOVA) results.

1. Introduction

The combination of strength and ductility of a steel is the most important property for the development of lightweight vehicles with lower fuel consumption and higher safety. As an advanced high strength steels (AHSS), Twinning Induced Plasticity (TWIP) steels with high manganese austenitic microstructure and high strain hardening capacity offer to fulfill this request. Early work on TWIP steels, which is discovered by Hadfield in 1988, was carried out late 1900's [1–4]. There are numerous studies about microstructural and mechanical properties, effect of alloying elements, strain hardening mechanism, heat treatments etc. of TWIP steels [3,5–8].

On the other hand, suitability for manufacturing process is another important property which materials should provide. For the automotive industry, welding, especially resistance spot welding (RSW), is a mandatory process for almost all body parts. Consequently, welding of TWIP steels became a significant issue for usage in automotive industry. Some researchers investigated laser welding (LW) [9–12], dissimilar welding [4,11,13], friction stir spot welding[14] and RSW [15–19] of TWIP steels. However, the effect of the welding parameters on the mechanical and microstructural properties and the optimization of the welding parameters for TWIP steels is not well studied.

IOP Conf. Series: Journal of Physics: Conf. Series **885** (2017) 012010 doi:10.1088/1742-6596/885/1/012010

Almost all studies were focused on only load bearing capacity of the welded joints. But, not only mechanical properties but also indentation has a vital importance for automotive industry. In this study, a multi objective optimization approach was conducted using tensile shear load and indentation values for RSW of 1.3 mm 1Gpa grade and %15 cold rolled TWIP steel sheets. The mechanical properties of the weld were examined by means of TST and micro hardness tests. Effects of the welding parameters on the RSWed joints were discussed.

2. Material and method

In this study, as-received (1.3 mm) TWIP steel sheets were cold rolled %15 in thickness (around 1.1 mm) using cold rolling. All experiments were conducted on %15 cold rolled TWIP steel sheets. The chemical composition of the sheets used in this study is shown in Table 1.

Table 1. The chemical compositions (wt.%) and mechanical properties of %15 cold rolled TWIP steel sheets used in this investigation.

Steel	Fe	C	Mn	Si	Al	Cr	Ti	Ultimate Tensile Strength (MPa)	Total Elongation (%)
TWIP	*Balance*	0.28	15.6	1.06	1.89	0.564	0.1	1220	20

TWIP steel sheets were resistance spot welded in the overlapped configuration using MFDC resistance spot-welding machine connected to ABB robot arm and copper alloy electrodes having the face diameter of 6 mm. Prior to welding experiments, in order to determine the range of focused process parameters for RSW (welding current, welding time and electrode force), preliminary tests were carried out. The accepted criteria for the preliminary tests were the smallest button in peeling test and a maximum %35 indentation value.

Taguchi approach based multi objective optimization was performed using L9 orthogonal array and the parameter values shown in Table 2. First, S/N ratios were calculated separately for maximizing the tensile shear load (TSL) and minimizing the indentation values. In this step, calculated S/N values were normalized using the following equation:

$$Normalized\ S/N = \frac{S/N_i - S/N_{min}}{S/N_{max} - S/N_{min}}$$

where S/Ni is the calculated S/N ratio for the ith performance characteristics.

Then, the values used in Taguchi optimization were calculated by averaging normalized S/N values of TSL and indentation. To determine the relative effect of the parameters ANOVA procedure was also performed using the normalized S/N ratio values.

3. Results and discussion

The tensile shear load and indentation values of welded samples were presented with calculated S/N ratios in Table 2. The calculated heat input index values were also shown in this Table. Additionally, to determine the influence of each level of the response tables were calculated and shown in Table 3. Delta values of the welding parameters shows the magnitude of the effect on response values and rank values shows the order of importance of the welding parameters. Table 3 indicates that the most influential welding parameter was welding current. Main effects plot for the normalized S/N ratios plotted using the values in Table 3 (Fig. 1). Predicted optimum levels of welding parameters were also indicated using asterisk.

Table 2. Welding parameters and their TSL, indentation, heat input index values and S/N ratios.

Sample No.	Electrode Force (N)	Weld Current (kA)	Welding Time (ms)	Heat Input Index*	TSL [kN]	Indentation [%]	Average of Normalized S/N Ratio of TSL and Indentation
1	1500	3	100	600	4.18	1.39	0.522
2	1500	6	250	6000	9.71	16.92	0.530
3	1500	9	400	21600	10.54	35.21	0.475
4	2250	3	250	1000	4.77	1.31	0.558
5	2250	6	400	6400	10.23	12.09	0.623
6	2250	9	100	3600	10.61	28.90	0.484
7	3000	3	400	1200	3.96	1.67	0.463
8	3000	6	100	1200	8.56	14.44	0.511
9	3000	9	250	6750	11.61	29.55	0.527

*Heat Input Index = I^2t/F (I: Weld current (A); t: Welding time(s); F: Electrode force (N))

Table 3. Response table for Normalized S/N Ratios.

	Means		
Level	**Electrode Force**	**Weld Current**	**Welding Time**
1	0.509	0.515	0.506
2	0.555*	0.555*	0.538*
3	0.500	0.495	0.520
Delta	0.055	0.059	0.033
Rank	**2**	**1**	**3**
* Optimum level			

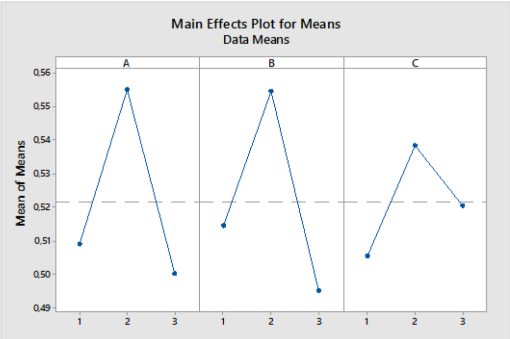

Figure 1. Main effects plot for the Normalized S/N Ratios.

According to Taguchi calculations, optimum levels of the welding parameters found to be 2250 N for welding force, 6 kA for welding current and 250 ms for welding time. Predicted optimum parameter set was not in the used orthogonal array, and thus, confirmation experimental test was required. To confirm the optimum levels of welding parameters, joining process was carried out again using predicted optimum parameter set and tensile shear load – deformation curves of selected samples having minimum, maximum and mean heat input index and optimum sample were presented in Fig 2. Obtained results of confirmation test were given in Table 4. The obtained maximum TSL was 11.61 kN (sample 9) with %29.55 indentation. Despite, %9.6 decrease in TSL, %59 decrease in indentation was achieved by optimization of welding parameters.

To determine the relative effect of the welding parameters and compare with Taguchi results, the standard ANOVA procedure was also performed using the normalized S/N ratios(Table 5). The most important parameter defined as weld current with a contribution of 29.22 percent. The order of importance was also in a good relationship with Taguchi result.

Table 4. Experimental results of confirmation test.

Electrode Force (N)	Weld Current (kA)	Welding Time (ms)	TSL (kN)	Indentation (%)
2250	6	250	10.49	12.00

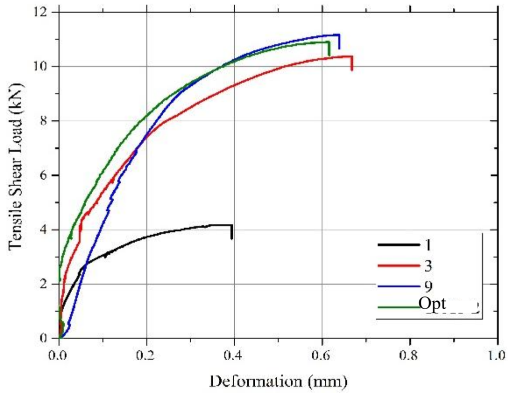

Figure 2. Tensile shear load – Deformation curves of selected samples.

Table 5. ANOVA table for normalized S/N ratios.

Source	DOF	Seq SS	Adj SS	Adj MS	F	Contribution (%)
Electrode Force	2	0.0052	0.0052	0.0026	0.79	27.51
Weld Current	2	0.0055	0.0055	0.0028	0.84	29.22
Welding Time	2	0.0016	0.0016	0.0008	0.25	8.57
Residual Error	2	0.0066	0.0066	0.0033		34.69
Total	8	0.0189				100.00

4. Conclusions

In this study, RSW welding parameters of cold rolled TWIP sheet steel joints have been multi-objectively optimized using Taguchi approach. Also, the effects of welding parameters were discussed by means of TST and indentation values of the joints. The main conclusions can be drawn as follows:

- Optimum levels of the welding parameters found to be 2250 N welding force, 6 kA welding current and 250 ms welding time.
- The order of importance of the welding parameters was found to be: weld current > electrode force > welding time.
- The sample welded using optimum parameter set showed %9.6 lower TSL and %59 lower indentation than the sample which has maximum TSL.

Acknowledgments

The authors are grateful to the Scientific and Technological Research Council of Turkey (TUBITAK) for its financial support to this research (Project number: MAG 213M597). The authors are also grateful to Ermetal Inc. for providing facilities for the resistance spot-welding processes.

References

[1] N. Zan, H. Ding, X. Guo, Z. Tang, W. Bleck, Effects of grain size on hydrogen embrittlement in a Fe-22Mn-0 . 6C TWIP steel, Int. J. Hydrogen Energy. 40 (2015) 1–10. doi:10.1016/j.ijhydene.2015.06.112.
[2] L. Halbauer, R. Zenker, A. Weidner, A. Buchwalder, H. Biermann, Electron Beam Welding of

Cold Rolled High-Alloy TRIP/TWIP Steel Sheets, Steel Res. Int. (2015) n/a–n/a. doi:10.1002/srin.201500086.

[3] Y. Zhao, J. Wang, S. Zhou, X. Wang, Effects of rare earth addition on microstructure and mechanical properties of a Fe–15Mn–1.5Al–0.6C TWIP steel, Mater. Sci. Eng. A. 608 (2014) 106–113. doi:10.1016/j.msea.2014.04.084.

[4] P. Russo Spena, M. De Maddis, F. Lombardi, M. Rossini, Dissimilar Resistance Spot Welding of Q&P and TWIP Steel Sheets, Mater. Manuf. Process. 31 (2016) 291–299. doi:10.1080/10426914.2015.1048476.

[5] T. Dieudonné, L. Marchetti, M. Wery, J. Chêne, C. Allely, P. Cugy, et al., Role of copper and aluminum additions on the hydrogen embrittlement susceptibility of austenitic Fe-Mn-C TWIP steels, Corros. Sci. 82 (2014) 218–226. doi:10.1016/j.corsci.2014.01.022.

[6] K. Renard, P.J. Jacques, On the relationship between work hardening and twinning rate in TWIP steels, Mater. Sci. Eng. A. 542 (2012) 8–14. doi:10.1016/j.msea.2012.01.123.

[7] J. Hajkazemi, a. Zarei-Hanzaki, M. Sabet, S. Khoddam, Double-hit compression behavior of TWIP steels, Mater. Sci. Eng. A. 530 (2011) 233–238. doi:10.1016/j.msea.2011.09.080.

[8] T. Declara, I. Cortes, N.A.S. Pens, E.S.D.E. Aposenta, D.E. Sobreviv, P.P. Cga, et al., Effect of heat treatment and hot working on the microstructural characteristics of TWIP steels, (2014) 1–81.

[9] L. Mujica, S. Weber, H. Pinto, C. Thomy, F. Vollertsen, Microstructure and mechanical properties of laser-welded joints of TWIP and TRIP steels, Mater. Sci. Eng. A. 527 (2010) 2071–2078. doi:10.1016/j.msea.2009.11.050.

[10] T. Wang, M. Zhang, W. Xiong, R. Liu, W. Shi, L. Li, Microstructure and tensile properties of the laser welded TWIP steel and the deformation behavior of the fusion zone, Mater. Des. 83 (2015) 103–111. doi:10.1016/j.matdes.2015.06.002.

[11] V. Behm, M. Höfemann, A. Hatscher, A. Springer, S. Kaierle, D. Hein, et al., Investigations on Laser Beam Welding Dissimilar Material Combinations of Austenitic High Manganese (FeMn) and Ferrite Steels, Phys. Procedia. 56 (2014) 610–619. doi:10.1016/j.phpro.2014.08.049.

[12] H. Li, H. Jiang, L. Yang, Y. Wang, Mechanical properties and microstructure of laser welded TWIP steels, Cailiao Kexue Yu Gongyi/Material Sci. Technol. 22 (2014) 6–9. http://www.scopus.com/inward/record.url?eid=2-s2.0-84925271057&partnerID=tZOtx3y1.

[13] P.R. Spena, P. Matteis, A. Sanchez, G. Scavino, Strength and fracture of TWIP steel dissimilar weld joints, Convegno IGF XXII Roma. (2013) 109–117. http://www.gruppofrattura.it/ocs/index.php/cigf/IGF22/paper/view/10900.

[14] M.M.Z. Ahmed, E. Ahmed, A.S. Hamada, S.A. Khodir, M.M. El-Sayed Seleman, B.P. Wynne, Microstructure and mechanical properties evolution of friction stir spot welded high-Mn twinning-induced plasticity steel, Mater. Des. (2015). doi:10.1016/j.matdes.2015.12.001.

[15] M.H.H. Razmpoosh, M. Shamanian, M. Esmailzadeh, The microstructural evolution and mechanical properties of resistance spot welded Fe – 31Mn – 3Al – 3Si TWIP steel, Mater. Des. 67 (2015) 571–576. doi:10.1016/j.matdes.2014.10.090.

[16] D.C. Saha, S. Han, K.G. Chin, I. Choi, Y. Do Park, Weldability evaluation and microstructure analysis of resistance-spot- welded high-Mn steel in automotive application, Steel Res. Int. 83 (2012) 352–357. doi:10.1002/srin.201100324.

[17] D.C. Saha, Y. Cho, Y. Park, Metallographic and fracture characteristics of resistance spot welded TWIP steels, 18 (2013) 711–720. doi:10.1179/1362171813Y.0000000151.

[18] P. Russo Spena, M. De Maddis, F. Lombardi, M. Rossini, Investigation on Resistance Spot Welding of TWIP Steel Sheets, Steel Res. Int. 86 (2015) 1480–1489. doi:10.1002/srin.201400336.

[19] J. Yu, J. Shim, S. Rhee, Characteristics of Resistance Spot Welding for 1 GPa Grade Twin Induced Plasticity Steel, Mater. Trans. 53 (2012) 2011–2018. doi:10.2320/matertrans.M2012167.